Petrology, Vol. 12, No. 1, 2004, pp. 70–81. Translated from Petrologiya, Vol. 12, No. 1, 2004, pp. 84–97.

Synthesis of Omphacites and Isomorphic Features of Clinopyroxenes in the System $CaMgSi_2O_6$–$NaAlSi_2O_6$–$KAlSi_2O_6$

O. G. Safonov*, Yu. A. Litvin*, and L. L. Perchuk**

**Institute of Experimental Mineralogy, Russian Academy of Sciences, Chernogolovka, Moscow oblast, 142432 Russia; e-mail oleg@iem.ac.ru*

***Faculty of Geology, Moscow State University, Vorob'evy gory, Moscow, 119899 Russia; e-mail llp@geol.msu.ru*

Received April 9, 2003

Abstract—Omphacites with varying Na/K ratio were synthesized in the system $CaMgSi_2O_6$–$NaAlSi_2O_6$–$KAlSi_2O_6$ at pressures of 5, 6, and 7 GPa within the temperature interval 1000–1300°C. It was found that both K and Na contents of omphacites increase irregularly with pressure, and there is a distinct negative correlation between K and Na in clinopyroxene at each pressure. The K content of omphacite increases more intensely within a pressure interval of 6–7 GPa. The isomorphism $Na^{M2} \rightleftarrows K^{M2}$ is predominant, whereas the substitution $[Ca^{M2}Mg^{M1}] \rightleftarrows [K^{M2}Al^{M1}]$ increases with decreasing jadeite content. At the *P–T* parameters studied, potassium-bearing omphacites coexist with melt containing 15–21 wt % K_2O, 54–63 wt % SiO_2, and 19–22 wt % Al_2O_3 at low Na_2O concentration independent of the initial Na_2O content in starting mixtures. The partition coefficients $K_p(K_2O) = K_2O$ (in *KCpx*)/K_2O (in melt) and $K_p(Na_2O) = Na_2O$ (in *KCpx*)/Na_2O (in melt) increase with pressure, and $K_p(Na_2O)$ increases more significantly by comparison to $K_p(K_2O)$. Thus, omphacite crystallization promotes melt enrichment in potassium. As a result, *ultrapotassic* mantle melts could be generated. This is exemplified by potassium-bearing omphacite inclusions in diamonds from kimberlite and lamproite pipes.

INTRODUCTION

Potassium-bearing omphacites of the system $CaMgSi_2O_6$–$NaAlSi_2O_6$–$KAlSi_2O_6$ (*Di*[1]–*Jd*–*KJd*) are common in mantle xenoliths from kimberlites and lamproites (McGregor and Carter, 1970; Reid *et al.*, 1976; Bishop *et al.*, 1978) and as inclusions in diamonds (Prinz *et al.*, 1975; Sobolev *et al.*, 1983; Moore and Gurney, 1985; Ricard *et al.*, 1989; Jaques *et al.*, 1989; Novgorodov *et al.*, 1990; Sobolev *et al.*, 1998; Stachel *et al.*, 2000). Potassium-bearing omphacites belong to the eclogitic paragenesis. In contrast to clinopyroxenes of the peridotitic paragenesis (e.g., Jaques *et al.*, 1990), they are characterized by low Cr_2O_3 content and high, up to 15 wt %, Al_2O_3 content. The K_2O content of omphacites of the eclogitic paragenesis may be as high as 1.2–1.5 wt % (*e.g.*, Jaques *et al.*, 1989; Stachel *et al.*, 2000) at wide Na_2O variations (up to 10 wt %). Potassium-bearing omphacites are usually associated with garnet, which shows elevated Na_2O concentration (Prinz *et al.*, 1975; Bishop *et al.*, 1978; Sobolev *et al.*, 1983) and a notable majorite fraction (Stachel *et al.*, 2000). Assemblages of potassium-bearing omphacites (containing from 0.62 to 0.87 wt % K_2O) with phlogopite, rutile, magnetite, corundum, and coesite were described (Prinz *et al.*, 1975; Sobolev *et al.*, 1998). Such clinopyroxenes were also found as inclusions in diamond together with potassium feldspar or potassic aluminosilicate glass (Prinz *et al.*, 1975; Novgorodov *et al.*, 1990; Sobolev *et al.*, 1998). The omphacite inclusions in diamond are notably richer in K_2O than omphacites from the eclogite matrix (e.g., Taylor *et al.*, 1996). The lowest K_2O concentrations (<0.2 wt %) were detected in omphacites from grospydites containing kyanite, coesite, and potassium feldspar (Smyth and Hatton, 1977; Schulze *et al.*, 2000). Potassium-bearing omphacites are rare in other rock types. There is only one finding of clinopyroxene megacrysts containing 0.65–2.34 wt % K_2O and 1.0–3.3 wt % Na_2O from the potassium-rich hawaiites of Western Australia (Ghorbani and Middlemost, 2000).

[1] The following notations were used in the paper. Mineral abbreviations: *Ab*, albite $NaAlSi_3O_8$; Ca-*Esk*, Eskola molecule $Ca_{0.5}AlSi_2O_6$; Ca-*Ts*, Tschermak molecule $CaAl_2SiO_6$; *Cen*, clinoenstatite $Mg_2Si_2O_6$; *Di*, diopside $CaMgSi_2O_6$; *Grt*, garnet; *Jd*, jadeite $NaAlSi_2O_6$; *KCpx*, potassium-bearing clinopyroxene; *Kfs*, potassium feldspar $KAlSi_3O_8$; *KJd*, potassium jadeite $KAlSi_2O_6$; *L*, melt; *Mc*, phengite-like micas; and *SWd*, Si-wadeite $K_2Si_4O_9$. Thermodynamic parameters: *T*, temperature, *C*; *P*, pressure, GPa; $K_p(Na_2O) = Na_2O^{KCpx}/Na_2O^{L}$, Na_2O (wt %) partition coefficient between potassium-bearing clinopyroxene and melt; $K_p(K_2O) = K_2O^{KCpx}/K_2O^{L}$, K_2O (wt %) partition coefficient between potassium-bearing clinopyroxene and melt; and ΔG_R, Gibbs free energy change of reaction *R*.

Table 1. Conditions and products of experiments on *KCpx* synthesis in the system $CaMgSi_2O_6$–$NaAlSi_2O_6$–$KAlSi_2O_6$

Run number	Composition of starting mixture, mol %			*T*, °C	*P*, GPa	Duration, min	Run products
	$CaMgSi_2O_6$	$NaAlSi_2O_6$	$KAlSi_2O_6$				
945	0	40	60	1200	7	450	*KCpx*, Glass
973	0	40	60	1000	5	780	*KCpx*, Glass
925	8	32	60	1300	7	360	*KCpx*, Glass
972	8	32	60	1100	5	430	*KCpx*, Glass
923	20	20	60	1300*	7	360	*KCpx*, *SWd*, *Mc*
983	20	20	60	1150	6	450	*KCpx*, *Grt*, Glass
971	20	20	60	1100	5	430	*KCpx*, Glass, *Mc*
924	32	8	60	1300*	7	360	*KCpx*, *Grt*, *Mc*
984	32	8	60	1170	6	400	*KCpx*, Glass, *Mc*
979	32	8	60	1100	5	430	*KCpx*, Glass, *Mc*
982	40	0	60	1100	5	430	*KCpx*, Glass

Note: *Mc*, phases similar in composition to phengite micas (see text).
* Samples were quenched in the regime of a gradual temperature decrease during 1.0–1.5 min; other samples were abruptly quenched.

These facts point to a wide range of conditions, under which natural Na–K-bearing clinopyroxenes are formed. Experimental studies demonstrated that variations in the concentrations of these components in clinopyroxene have a direct bearing on the pressure of crystallization and alkalinity of coexisting melts and fluids (e.g., Kushiro, 1965; Harlow, 1997; Perchuk *et al.*, 2002). Natural clinopyroxenes show a negative correlation between K and Na (e.g., Sobolev *et al.*, 1998).

Potassium-bearing omphacites were repeatedly synthesized at $P > 5$ GPa in experiments on the melting of natural potassic rocks, such as lamproites (see a review in Perchuk *et al.*, 2002). The maximum K_2O content of experimental clinopyroxene reached 1.8–2.6 wt % at an Na_2O content of up to 4 wt %. Omphacites containing up to 3.7 wt % K_2O were synthesized in the systems *Di–Kfs–Ab* and *Di–Jd–Kfs* at pressures of 9.5–11 GPa (Harlow, 1999). The most comprehensive experimental data on potassium solubility in jadeite-rich clinopyroxene were obtained by Harlow (1997), who studied clinopyroxene equilibrium with potassic carbonate melt at 10 GPa. These experiments showed that $KAlSi_2O_6$ solubility in jadeite is appreciably lower than in diopside and omphacite. Harlow (1997) assumed that low concentrations of the small Na cation could stabilize the clinopyroxene structure compensating the unit-cell expansion related to incorporation of large potassium. In other words, low sodium concentrations could be favorable for potassium incorporation in clinopyroxene. Unfortunately, such data exist only for 10 GPa (Harlow, 1997).

There are no systematic data on potassium solubility in omphacites at other pressures. However, the existence of distinct opposite dependencies of K content in clinopyroxene on pressure and Na content may be very important for the estimation of relative depth of natural clinopyroxene crystallization (e.g., Sobolev *et al.*, 1998). The purpose of our experiments was the synthesis of solid solutions in the model system $CaMgSi_2O_6$–$NaAlSi_2O_6$–$KAlSi_2O_6$ in order to study systematically the dependence of Na–K isomorphism in clinopyroxene in equilibrium with aluminosilicate melt on pressure and jadeite content with application to natural clinopyroxenes.

STARTING MATERIALS, EXPERIMENTAL AND ANALYTICAL TECHNIQUES

Mixtures of $CaMgSi_2O_6$, $NaAlSi_2O_6$, and $KAlSi_2O_6$ gels prepared by the nitrate method (Hamilton and Henderson, 1968) were used as starting materials for our experiments. All the experimental mixtures contained 60 mol % $KAlSi_2O_6$ and varying amounts $CaMgSi_2O_6$ and $NaAlSi_2O_6$ (Table 1). The choice of such a system composition was conditioned by the results of our experiments on *KCpx* synthesis in the system $CaMgSi_2O_6$–$KAlSi_2O_6$ (Safonov *et al.*, 2002). These experiments showed that 60 mol % $KAlSi_2O_6$ in the system was the most favorable for the synthesis of compositionally homogeneous euhedral *KCpx* crystals. High $KAlSi_2O_6$ content in the starting mixture provides conditions for homogeneous K and Al distribution, which are necessary for generation of the $KAlSi_2O_6$ end-member in the newly formed clinopyroxene. *KCpx* crystals are usually very heterogeneous at low $KAlSi_2O_6$ content in the system. At higher $KAlSi_2O_6$ content in the starting mixture, *KCpx* may be unstable, and garnet crystallizes instead of clinopyroxene (Safonov *et al.*, 2002). The gels were mixed under alcohol in accordance with the target system compositions. About 20 mg of the mixtures were placed into

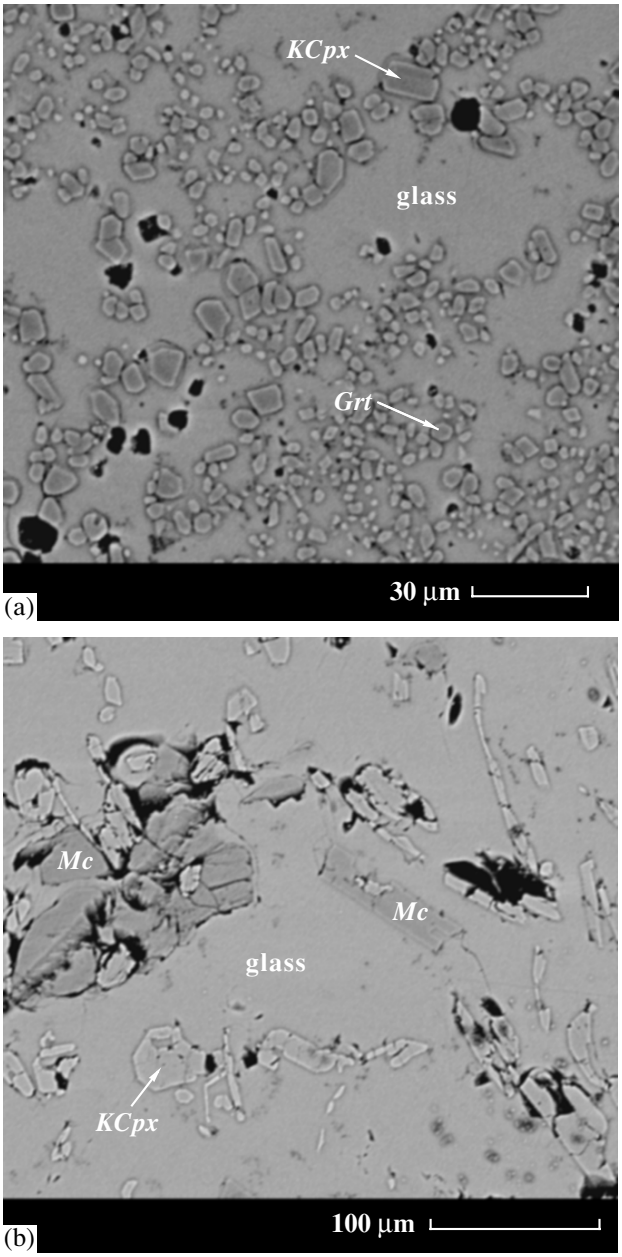

Fig. 1. Relationships of *KCpx* crystals with coexisting phases in the experimental products in the system $CaMgSi_2O_6$–$NaAlSi_2O_6$–$KAlSi_2O_6$. Back-scattered electron images, CamScan electron microscope.

(a) Euhedral crystals of *KCpx* and *Grt* in homogeneous aluminosilicate glass from products of run 983 (Table 1). (b) *KCpx* crystals and flakes of phengite-like mica (*Mc*) in homogeneous aluminosilicate glass in the products of run 971 (Table 1). Dark areas in the glass are clusters of tiny crystals of kyanite or corundum.

$Pt_{60}Rh_{40}$ capsules, which were dried for 12–15 hours at a temperature of 110°C and welded shut. Despite the prolonged drying, the charges contained some water. The presence of water resulted in the formation of hydrous phases in the run products (see below).

The experiments were performed using a high-pressure apparatus of the *anvil-with-hole* type, which is characterized by homogeneous pressure and temperature distribution inside the reactor (Litvin, 1991) with a working volume of 0.10–0.15 cm^3. The experimental cells consisted of toroidal gaskets manufactured from lithographic limestone and graphite heaters, 7.2 mm in length, 7.5 mm in diameter, and 1.5 mm in wall thickness. Details of the cell assembly and pressure and temperature calibration were given by Safonov *et al.* (2002). Pressure was controlled with an accuracy of ±0.1 GPa. Temperature was monitored by a MINITH-ERM-300.31 regulator with an accuracy of ±20°C using the calibrated heating power–temperature dependency.

Experimental conditions are shown in Table 1. After experiments, samples were mounted in epoxy. The texture of the experimental samples was examined in reflected light and under a CamScan electron microscope at the Department of Petrology, Moscow State University. Phase compositions were analyzed using an electron microprobe with an EDS Link AN10/85S system at the departments of Petrology and Mineralogy, Moscow State University. Analyses were obtained at 15 kV accelerating potential and 3 μm electron beam diameter. Glasses (or quench products) were analyzed with a defocused beam or by scanning over an area of 10×10 μm. The maximal discrepancy in oxide content obtained by different equipments did not exceed ±2 wt %.

Mineral formulas were normalized to certain numbers of oxygen atoms. The distribution of components among the structural sites of clinopyroxene was calculated using the following scheme: $Al^T = 2 - (Si)$, $Al^{M1} = (Al) - Al^T$, $Mg^{M1} = 1 - Al^{M1}$, $Mg^{M2} = (Mg) - Mg^{M1}$, and $\square^{M2} = 1 - Ca - K - Mg^{M2}$, where components in parentheses denote their contents in formulas normalized to 6 oxygen atoms.

EXPERIMENTAL RESULTS

Phase Assemblages of the Samples

The phase assemblages of experimental samples are shown in Table 1. All samples contain euhedral clinopyroxene crystals (Figs. 1a, 1b), 10–100 μm in size. Euhedral crystals up to 300 μm in size were produced in runs 972 and 973 (Table 1). In some $CaMgSi_2O_6$-rich samples synthesized at 6 and 7 GPa (runs 923, 924, and 983; Table 1), *KCpx* coexists with *Grt* (Fig. 1a) or *SWd*. The formation of *SWd* resulted from $KAlSi_2O_6$ decomposition at a pressure of 7 GPa (Safonov *et al.*, 2002). These phases are absent in sodium-rich experimental products in the system $CaMgSi_2O_6$–$KAlSi_2O_6$–$NaAlSi_2O_6$ (Table 1). They are also absent at 5 GPa. Flakes of a K–Al–Mg-phase, similar to that obtained in experiments in the system $CaMgSi_2O_6$–$KAlSi_2O_6$ (Safonov *et al.*, 2002), were found in samples 923, 971, 924, 984, and 979 (Table 1). All experimental products contain aluminosilicate glass or quench products (Table 1;

Figs. 1a, 1b). Homogeneous glass is characteristic of the $NaAlSi_2O_6$-rich samples and the samples synthesized at 6 and 5 GPa (Table 1) using a regime of rapid quenching. In some cases, partial glass crystallization produced clusters of tiny corundum or kyanite crystals (Fig. 1b). Fine-grained aggregates of K–Al–Mg-phases formed instead of glass at relatively slow quenching. This was observed in runs 923 and 924 (Table 1) performed at 7 GPa with $CaMgSi_2O_6$-rich mixtures. Homogeneous glass was absent in the products of these experiments.

Composition of Phases Accompanying Potassium-Bearing Omphacite

The compositions of clinopyroxenes and accompanying phases (*Grt*, *SWd*, aluminosilicate glass, and quench products) are presented in Table 2. The composition of garnet is highly variable: $X_{Ca} = Ca/(Ca + Mg)$ varies from 0.23–0.27 in sample 983 to 0.53–0.67 in sample 924. The composition of Si-wadeite in sample 923 (Table 1) is close to the theoretical formula $K_2Si_4O_9$ (Table 2). The composition of K–Al–Mg mica-like phases corresponds to phengite with varying Si content (Table 2). The highest Si content (up to 3.7 f.u. per 11 oxygen atoms) was observed in micas from the products of experiments at 7 GPa. The Si contents of micas produced at 6 and 5 GPa are similar and vary from 3.0 to 3.1 f.u. per 11 oxygen atoms. A decrease in Si content is accompanied by a regular increase in Mg at an approximately constant Al content. The SiO_2 content of glasses increases with increasing pressure from 54–59 wt % at 5 GPa to 58–63 wt % at 6 and 7 GPa. The Al_2O_3 (19–22 wt %) and K_2O (17–20 wt %) contents are relatively constant. Glasses produced at 7 GPa contain less then 1 wt % Na_2O. The Na_2O content of glasses produced at 5 GPa reaches 4 wt % (Table 2). The glass composition varies insignificantly with variations in the $NaAlSi_2O_6/CaMgSi_2O_6$ ratio in the system at 6 and 7 GPa. At 5 GPa there are appreciable variations in the Na_2O content of glasses (Table 2).

Clinopyroxene Composition and Characteristics of Na–K–Ca Isomorphism

The clinopyroxene crystals are relatively homogeneous. For an average K_2O content in some individual crystals of 1–2 wt %, variations in this component do not exceed 0.3 wt %. However, large crystals are usually zoned. The zoning is manifested by a decrease in K_2O content from center to rim of a crystal. Therefore, the compositions of centers of large crystals with notably higher K_2O contents were ignored when the average (presumably, equilibrated) K_2O content of omphacite was calculated (Table 2).

All synthesized pyroxenes show $K + Na \le Al$, a positive correlation between K + Na in the M2 site and the difference between Al in the M1 site (Al^{M1}) and Al in the tetrahedral coordination (Al^{IV}) (i.e., accounting for Ca-*Ts*), and a negative correlation between K + Na and Ca in the M2 site (Figs. 2a, 2b). These relations reflect *Jd* and *KJd* substitutions in the *KCpx* solid solution. All the pyroxenes synthesized are characterized by low Mg in the M2 site (Table 2), which corresponds to a small *Cen* content. The Al^{IV} content of clinopyroxene decreases regularly with increasing pressure. For example, *KCpx* from the products of 5-GPa experiments show significantly higher Al^{IV} contents (up to 0.16 f.u. per 6 oxygen atoms) as compared to *KCpx* produced at 7 GPa (Table 2). Nevertheless, all pyroxene analyses show an excess of Al^{M1} ($Al' = Al^{M1} - K - Na - Al^{IV}$) compared to Ca-*Ts*, *Jd*, and *KJd* compositions, which implies the presence of the Ca-*Esk* component in clinopyroxene. The presence of the Ca-Eskola molecule is supported by the calculated amount of vacancies ($\square = 1 - Ca - K - Na - Mg^{M2}$) in the M2 site, which is proportional to Al' concentration with a ratio of 1 : 2 in correspondence with the stoichiometry of the end-member $(Ca_{0.5}\square_{0.5})^{M2}Al^{M1}Si_2O_6$ (Fig. 2c). Potassium-bearing jadeites also contain excess Al in the M1 site and calculated vacancies in the M2 site. However, in contrast to omphacites, the direct correlation between $(Al')^{M1}$ and $\square^{M2}$ in jadeites is characterized by a slope of 1 : 1 (Fig. 2c). The occurrence of vacancies in the clinopyroxene structure in the system $NaAlSi_2O_6$–$KAlSi_2O_6$ can be related to the presence of OH groups. The concentration of these groups increases at high pressure, especially in Na-rich clinopyroxenes (Skogby *et al.*, 1990; Smyth *et al.*, 1991; Bromiley and Keppler, 2002). For comparison, Fig. 2c shows data points of natural hydrous omphacites (up to 9 wt % Na_2O). The presence of OH groups in these omphacites was established by IR spectrometry (Smyth *et al.*, 1991). The data points plot in this diagram along the line $(Al')^{M1} : (\square)^{M2} = 1 : 1$.

The average Na content in *KCpx* directly depends on the $NaAlSi_2O_6/CaMgSi_2O_6$ ratio of starting mixture. At constant pressure a negative correlation between K and Na is observed (Fig. 3a). Since K + Na shows a negative correlation with Ca, the predominant scheme of potassium substitution in jadeite-rich potassium-bearing pyroxene is $Na^{M2} \rightleftharpoons K^{M2}$. The isomorphism $Mg^{M1}Ca^{M2} \rightleftharpoons Al^{M1}K^{M2}$ known for pyroxenes of the system $CaMgSi_2O_6$–$KAlSi_2O_6$ (*e.g.* Safonov *et al.*, 2002) is of minor importance. The negative correlation between K and Na in omphacites is also confirmed by the opposite correlations of these components with Mg and Al, which occur in the M1 site (Figs. 3b, 3c). The K content of sodium-free *KCpx* does not exhibit a positive correlation with Mg and a negative correlation with Al (e.g., Safonov *et al.*, 2002).

Both Na and K concentrations of clinopyroxene increase with pressure. The negative correlation between these parameters at any given pressure is illustrated by isobars in the diagram (Fig. 3a). The 6 and 7 GPa isobars are parallel to each other and to the

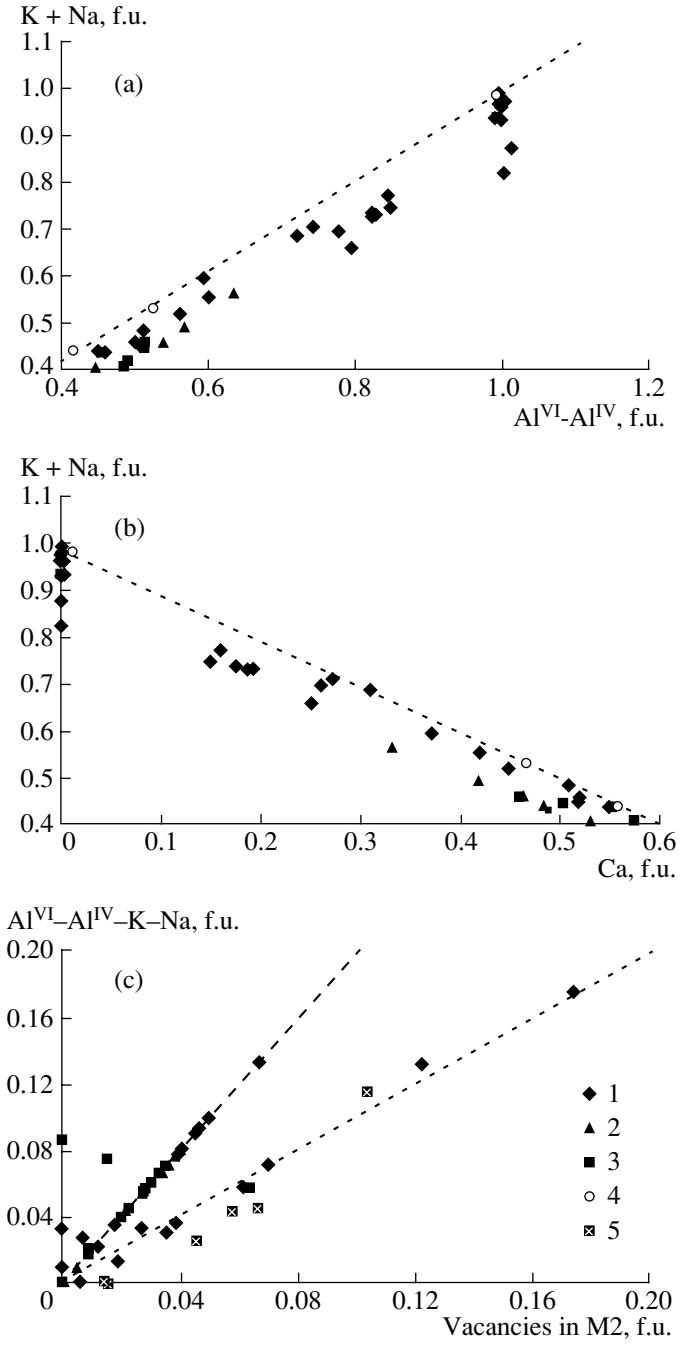

Fig. 2. Compositional features of the *KCpx* solid solutions synthesized in the system $CaMgSi_2O_6$–$NaAlSi_2O_6$–$KAlSi_2O_6$ at (1) 7 GPa, (2) 6 GPa, (3) 5 GPa, and (4) *KCpx* produced in the system *Di–Jd*–potassium carbonate at a pressure of 10 GPa (Harlow, 1997).
(a) Positive correlation of $K^{M2} + Na^{M2}$ with Al^{M1} (accounting for the Ca-*Ts* component), which indicates the presence of the *Jd* and *KJd* end-members in clinopyroxene. The dashed line corresponds to the theoretical scheme of the coupled substitution $Mg^{M1} + Ca^{M2} \rightleftharpoons Al^{M1} + (Na, K)^{M2}$. (b) Negative correlation of $K^{M2} + Na^{M2}$ with Ca^{M2}. The dashed line reflects the theoretical scheme of the coupled substitution $Mg^{M1} + Ca^{M2} \rightleftharpoons Al^{M1} + (Na, K)^{M2}$. (c) Positive correlation of the calculated amount of vacancies in the M2 site with the excess Al^{M1} (subtracting *Jd*, *KJd*, and Ca-*Ts* components), which indicates the presence of the Ca-*Esk* component in clinopyroxene. The dashed line corresponds to the theoretical scheme of the coupled substitution $Mg^{M1} + 0.5Ca^{M2} \rightleftharpoons Al^{M1} + 0.5\square^{M2}$ in the binary *Di*–Ca-*Esk* solution. The dotted line shows the positive correlation of the calculated amount of vacancies with the excess Al^{M1} in potassium-bearing jadeites (runs 945 and 973; Table 1). Also shown are (5) the compositions of natural OH-bearing omphacites (Smyth *et al.*, 1991).

Table 2. Average analyses of potassium-bearing omphacites and accompanying phases produced in experiments in the system $CaMgSi_2O_6$–$NaAlSi_2O_6$–$KAlSi_2O_6$ at 5, 6, and 7 GPa (Table 1)

Component	923			924			925		945		971		
	KCpx	*SWd*	*Mc*[3]	*KCpx*	*Grt*	*Mc*	*KCpx*	glass	*KCpx*	glass	*KCpx*	glass	*Mc*
	3[1]	2	1	5	2	3	8	6	8	5	6	1	5
SiO_2	57.92 (0.22)[2]	71.88	55.20	56.64 (0.21)	42.17	55.40	57.94 (0.86)	58.92	59.93 (0.38)	61.95	55.68 (0.50)	58.33	45.61
Al_2O_3	18.74 (0.68)	0.29	22.06	12.67 (1.19)	23.30	21.73	19.98 (2.48)	21.67	25.23 (0.22)	19.12	14.78 (1.14)	19.40	21.38
MgO	4.74 (0.36)	0.03	5.70	9.34 (0.74)	11.11	5.43	4.77 (1.73)	0.29	0.00	0.00	9.05 (0.78)	0.57	18.14
CaO	7.62 (0.68)	0.04	0.06	13.77 (1.10)	23.08	0.00	6.47 (2.69)	0.16	0.00	0.00	14.07 (1.29)	0.74	0.04
Na_2O	9.48 (0.26)	0.03	0.00	5.46 (0.59)	0.08	0.00	9.74 (1.62)	0.66	14.35 (0.56)	0.43	6.19 (0.45)	1.29	0.10
K_2O	1.49 (0.17)	27.73	11.98	2.02 (0.29)	0.26	12.27	1.10 (0.53)	18.27	0.41 (0.14)	18.42	0.26 (0.08)	19.66	12.26
Total	99.99	100.00	95.00	99.99	100.00	94.83	100.00	100.01	99.92	99.92	100.03	100.03	97.53
Formula units recalculated for the given number of oxygen atoms													
O	6	9	11	6	12	11	6	24	6	24	6	24	11
Si	1.993	3.992	3.667	1.987	3.030	3.692	1.982	8.368	2.012	8.749	1.940	8.414	3.059
Al	0.760	0.019	1.727	0.524	1.972	1.705	0.806	3.623	0.998	3.181	0.607	3.298	1.690
Mg	0.243	0.002	0.564	0.493	1.189	0.537	0.243	0.060	0.000	0.000	0.470	0.122	1.813
Ca	0.281	0.002	0.004	0.517	1.776	0.000	0.237	0.024	0.000	0.000	0.525	0.115	0.003
Na	0.632	0.003	0.000	0.371	0.011	0.000	0.645	0.182	0.934	0.117	0.418	0.362	0.013
K	0.065	1.964	1.015	0.090	0.024	1.044	0.048	3.307	0.017	3.318	0.012	3.616	1.048
Total	3.974	5.982	6.977	3.982	8.002	6.978	3.961	15.564	3.961	15.365	3.972	15.927	7.626
Distribution of components in the crystal chemical sites of *KCpx*[4]													
Al^{IV}	0.006			0.013			0.018		0.000		0.060		
Al^{M1}	0.754			0.511			0.788		0.998		0.547		
Mg^{M1}	0.243			0.489			0.212		0.000		0.453		
Mg^{M2}	0.000			0.003			0.031		0.000		0.017		
$□^{M2}$	0.021			0.018			0.038		0.047		0.029		
$K_p(K_2O)$[5]	?			?			0.06		0.02		0.01		
$K_p(Na_2O)$[6]	?			?			14.75		33.37		4.80		

Table 2. (Contd.)

Component	972		973		979			983			984		
	KCpx	glass	*KCpx*	glass	*KCpx*	glass	*Mc*	*KCpx*	*Grt*	glass	*KCpx*	glass	*Mc*
	3	2	1	1	4	1	2	8	2	2	3	1	1
SiO_2	52.61 (0.54)	54.66	60.30	57.73	54.54 (0.27)	59.56	43.77	55.54 (0.95)	44.00	61.95	56.45 (1.07)	61.12	45.23
Al_2O_3	15.21 (1.12)	21.49	25.19	22.18	8.10 (0.24)	20.38	19.32	17.14 (1.15)	24.03	20.41	7.54 (0.99)	20.33	19.79
MgO	11.39 (0.55)	2.07	0.00	0.00	13.25 (1.12)	0.46	16.81	8.15 (0.67)	21.42	0.68	14.10 (0.55)	1.57	19.94
CaO	16.57 (0.41)	1.93	0.00	0.00	21.04 (0.75)	0.33	0.58	11.70 (1.61)	9.99	0.20	18.12 (1.46)	1.54	0.00
Na_2O	4.17 (0.37)	4.19	14.41	3.61	2.33 (0.25)	0.59	0.00	6.81 (0.74)	0.24	0.71	2.20 (0.17)	0.75	0.00
K_2O	0.05 (0.02)	15.66	0.04	16.35	0.63 (0.06)	18.68	12.14	0.65 (0.12)	0.31	16.04	1.59 (0.66)	14.68	11.89
Total	100.00	100.00	99.94	99.87	99.89	100.00	92.62	99.99	99.99	99.99	100.00	99.99	96.85
Formula units recalculated for the given number of oxygen atoms													
O	6	24	6	24	6	24	11	6	12	24	6	24	11
Si	1.847	7.879	2.019	8.210	1.944	8.475	3.105	1.926	3.043	8.638	1.995	8.516	3.087
Al	0.629	3.650	0.994	3.317	0.340	3.417	1.615	0.700	1.958	3.354	0.314	3.338	1.557
Mg	0.596	0.444	0.000	0.000	0.704	0.098	1.776	0.421	2.207	0.142	0.724	0.326	1.983
Ca	0.623	0.298	0.000	0.000	0.803	0.050	0.044	0.435	0.740	0.031	0.686	0.230	0.000
Na	0.284	1.170	0.935	0.994	0.161	0.164	0.000	0.457	0.032	0.191	0.151	0.202	0.000
K	0.002	2.880	0.002	2.966	0.029	3.389	1.098	0.029	0.027	2.851	0.072	2.608	1.013
Total	3.981	16.321	3.95	15.487	3.981	15.593	7.638	3.968	8.007	15.207	3.942	15.220	7.640
Distribution of components in the crystal chemical sites of *KCpx*[4]													
Al^{IV}	0.153		0.000		0.056			0.074			0.005		
Al^{M1}	0.476		0.994		0.284			0.626			0.309		
Mg^{M1}	0.524		0.000		0.704			0.374			0.691		
Mg^{M2}	0.072		0.000		0.000			0.047			0.051		
$\square^{M2}$	0.019		0.063		0.007			0.033			0.041		
$K_p(K_2O)$[5]	0.003		0.002		0.03			0.04			0.11		
$K_p(Na_2O)$[6]	0.99		3.99		3.95			9.59			2.93		

Note: [1] Number of individual analyses; [2] standard deviations of oxide contents in clinopyroxene are shown in parentheses; [3] mica-like phases close to phengite in composition (see text); [4] see text for the scheme of calculation; [5] K_p (K_2O) = K_2O (*Cpx*)/K_2O (glass); [6] K_p (Na_2O) = Na_2O (*Cpx*)/Na_2O (glass).

10 GPa isobar constructed on the basis of experimental data in the system omphacite–carbonate melt (Harlow, 1997). The 5 GPa isobar has a gentler slope (Fig. 3a), which implies that some other factor limits the solubility of the $KAlSi_2O_6$ end-member in omphacite. This factor is the higher content of Ca-*Ts* in *KCpx* synthesized at 5 GPa. This suggestion is supported by the notable deviation of *KCpx* compositions from run 972 (Table 1) from the 5 GPa isobar (Fig. 3a). This *KCpx* is characterized by the highest Al^{IV} content (0.13–0.16 f.u., Table 2).

Figure 3a illustrates an irregular increase of potassium content in *KCpx* with increasing pressure. The diagram shows that the 5 and 6 GPa isobars are close to each other, which suggests a relatively weak pressure influence on *KJd* solubility in omphacite (0.04–0.01 f.u. per GPa). A similar effect is also characteristic of the pressure interval 7–10 GPa (0.004–0.003 f.u. per GPa). The potassium jadeite content of the ternary solid solution increases significantly only within 6–7 GPa (0.06–0.05 f.u. per GPa).

DISCUSSION AND APPLICATION TO NATURAL ASSEMBLAGES

Factors Controlling $KAlSi_2O_6$ Solubility in Omphacite in Equilibrium with Aluminosilicate Melt

The solubility of K-jadeite component in omphacite is controlled by both the composition of coexisting melt (activities of components) and the composition of clinopyroxene (jadeite content). In the starting mixtures of all experiments, $KAlSi_2O_6$ concentration was constant and high (60 mol %). Thus, variations in the K content of *KCpx* at constant *P* and *T* are not related to variations in $KAlSi_2O_6$ in the system. At constant *P* and *T*, the concentrations of SiO_2 and Al_2O_3 in the melt only slightly vary with changes in the $NaAlSi_2O_6/CaMgSi_2O_6$ ratio of the system (Table 2). Therefore, the activities of these components in the melt could not be the factor strongly influencing $KAlSi_2O_6$ solubility in omphacite under conditions of our experiments. This conclusion is supported by the fact that the limiting influence of jadeite component on potassium content is also observed in *KCpx* synthesized in equilibrium with carbonate melts with low SiO_2 and Al_2O_3 concentrations (Harlow, 1997). The Na_2O content in the melt varies insignificantly at pressures of 6 and 7 GPa with changes in the $NaAlSi_2O_6/CaMgSi_2O_6$ ratio of the system. The average content of jadeite component in *KCpx* directly depends on the $NaAlSi_2O_6/CaMgSi_2O_6$ ratio in the starting mixture. These relations show that Na_2O activity in melt is also not a major control on $KAlSi_2O_6$ solubility in omphacite at lest at 6 and 7 GPa. The jadeite content (activity) of clinopyroxene is a major factor responsible for regular changes in K-jadeite content in omphacite. In other words, the crystal chemical factor is more important

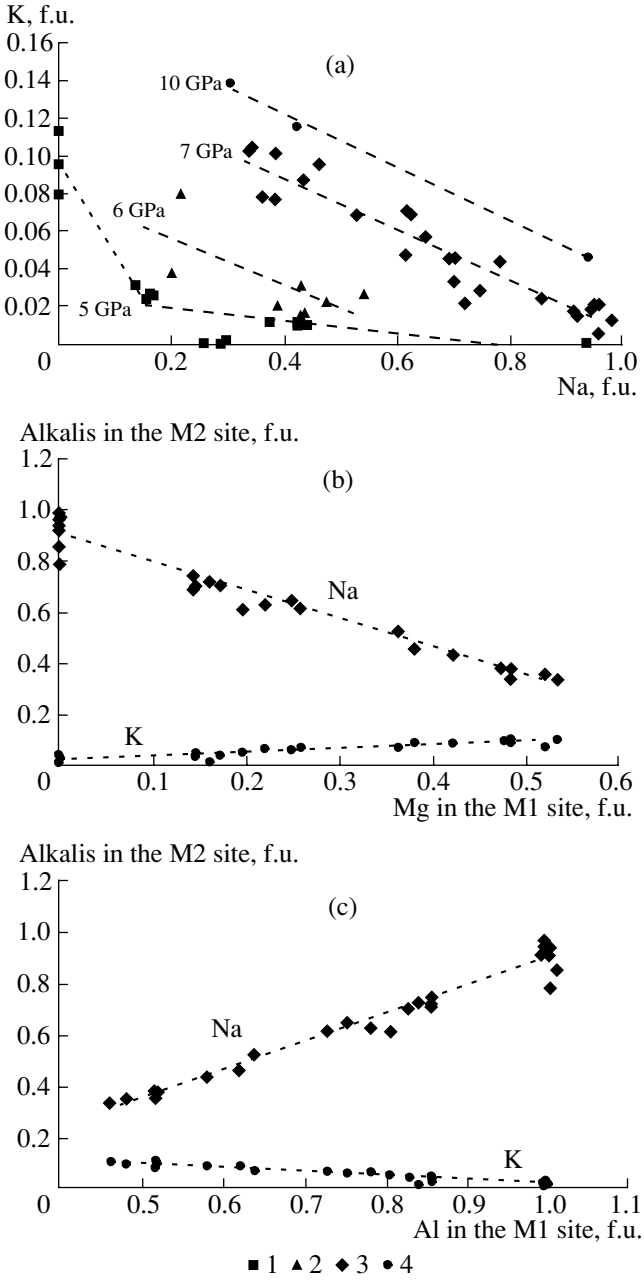

Fig. 3. Peculiarities of K–Na isomorphism in the solid solutions of potassium-bearing omphacites synthesized in the system $CaMgSi_2O_6$–$NaAlSi_2O_6$–$KAlSi_2O_6$.

(a) The influence of pressure and the limiting influence of the jadeite component on K substitution into omphacites at pressures of (1) 5 GPa, (2) 6 GPa, (3) 7 GPa, and (4) 10 GPa. Data for 10 GPa are taken from Harlow (1997). The dashed lines illustrate the limiting influence of the Na-component on the solubility of the K-component. The dotted line shows a relative abrupt increase in K solubility in Na-free *KCpx* at 5 GPa (run 982, Table 1). A similar jump was observed at 7 GPa (Safonov *et al.*, 2002). (b) Opposite directions of correlations of K^{M2} and Na^{M2} with Mg^{M1} (dashed lines) in *KCpx* synthesized at 7 GPa. (c) Opposite direction of correlations of K^{M2} and Na^{M2} with Al^{M1} (dashed lines) in *KCpx* synthesized at 7 GPa.

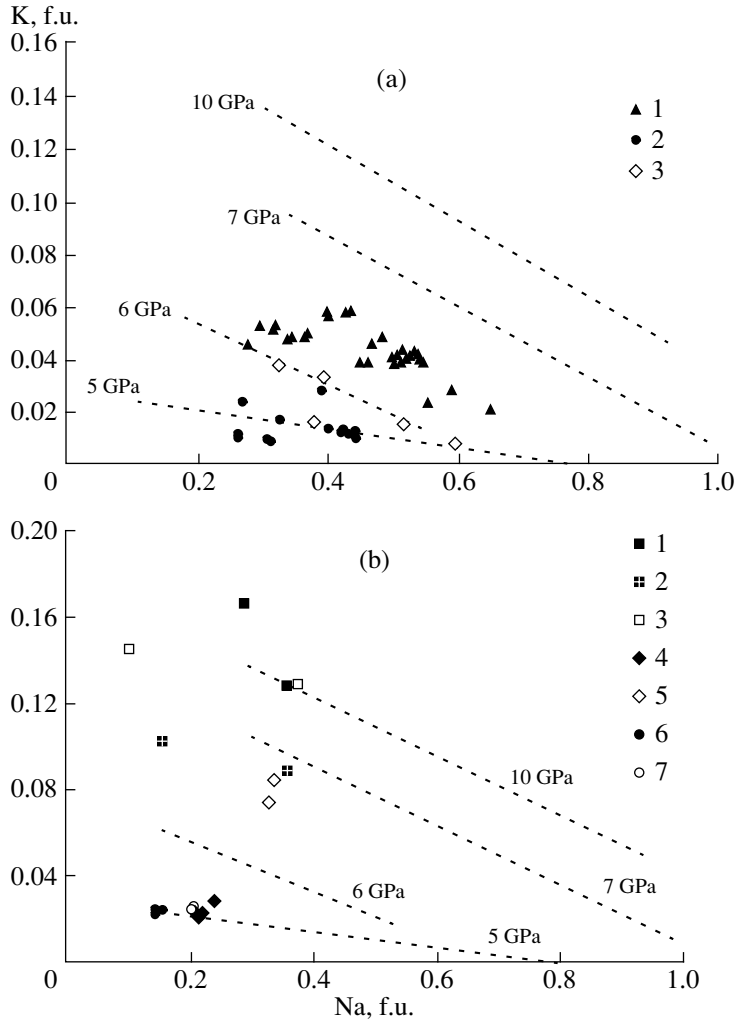

Fig. 4. Comparison of our experimental data on the potassium substitution into omphacites with (a) natural data and (b) results of other experimental studies. (a) (1) *KCpx* inclusions in diamonds from the Argyle pipe, Western Australia (Jaques *et al.*, 1989); (2) *KCpx* inclusions in diamonds from the Mir pipe (Sobolev *et al.*, 1983); (3) *KCpx* inclusions in diamonds from the Guaniamo region, Venezuela (Sobolev *et al.*, 1998). (b) (1)–(3) *KCpx* synthesized in the system $Di_{50}Jd_{50}$ + *Kfs* at (1) 9.5 GPa, (2) 10 GPa, and (3) 11 GPa (Harlow, 1999); (4)–(5) *KCpx* synthesized from the melt of sanidine–phlogopite lamproite at (4) 5 GPa and (5) 7 GPa (Mitchell, 1995); (6)–(7) *KCpx* synthesized from the melt of armalcolite–phlogopite lamproite at (6) 5 GPa and (7) 6 GPa (Edgar and Vukadinovic, 1993).

than the factor of melt composition, at least, under conditions of our experiments.

Crystal Chemical and Thermodynamic Reasons for the Limiting Influence of Jadeite Content on Potassium Incorporation in Clinopyroxene

The crystal chemical reason for the limiting influence of Na on the incorporation of the large K cation into the clinopyroxene structure is related to a significant decrease in unit-cell volume in the sequence diopside (~438 Å^3)–jadeite (~401 Å^3) (Wood *et al.*, 1980). However, Harlow (1997) suggested that this effect took place only at high Na concentrations. At relatively low Na concentrations, this component stabilizes the clinopyroxene structure compensating an increase in unit-cell volume due to large K incorporation, which is favorable for K substitution into the pyroxene lattice. Harlow's (1997) suggestion is valid for chromium-bearing *KCpx* synthesized in the system $CaMgSi_2O_6$–$NaCrSi_2O_6$–K-carbonate (Fig. 3 of Harlow, 1997). In contrast, omphacites synthesized in the system $CaMgSi_2O_6$–$NaAlSi_2O_6$–K-carbonate (Harlow, 1997) show a negative correlation between K and Na within the whole range of composition and pressure. This is in agreement with the results of our experiments (Fig. 3a). The problem of different K and Na behavior in omphacites and clinopyroxenes of the $CaMgSi_2O_6$–$NaCrSi_2O_6$ series is beyond the scope of the present study.

The limiting role of the jadeite component on *KJd* solubility in the *Di–Jd–KJd* solid solution can also be explained in the context of a change in the isomorphic scheme depending on jadeite content. Let us compare the specific features of the *Di–Jd*, *Di–KJd*, and *Di–Jd–KJd* solid solutions.

The nonideality of the binary *Di–Jd* solid solution (Gasparik, 1985) is related to the displacement to the left of the hypothetical internal exchange equilibrium (Wood *et al.*, 1980):

$$[CaMg]Si_2O_6 + [NaAl]Si_2O_6 = [CaAl]Si_2O_6 + [NaMg]Si_2O_6 \quad (1)$$

in the case of cation ordering between the M1 and M2 sites of the clinopyroxene structure. According to Wood *et al.* (1980), $\Delta G^0_{(1)}$ is about 22.8 kJ/mol. A positive $\Delta G_{(1)}$ corresponds to the isomorphism $Mg^{M1}Ca^{M2} \rightleftharpoons Al^{M1}Na^{M2}$. The *Di–KJd* solid solution is very limited even at high pressure. For example, at a pressure of 7 GPa, the maximum *KJd* solubility in diopside is 20–25 mol % (Chudinovskikh *et al.*, 2001; Safonov *et al.*, 2002). At a higher *KJd* concentration, the solid solution is unstable because of the reaction $3Di + 4KJd = Grt + 2SWd$ (Safonov *et al.*, 2002). In addition, the *Di–KJd* solid solution displays a distinct negative correlation between K^{M2} and Mg^{M1} and a positive correlation between K^{M2} and Al^{M1}, which indicates the isomorphism $Mg^{M1}Ca^{M2} \rightleftharpoons Al^{M1}K^{M2}$. From the point of view of the theory of reciprocal multisite solutions, these correlations imply a displacement to the left (positive ΔG_0) of the hypothetical internal exchange equilibrium similar to reaction (1):

$$[CaMg]Si_2O_6 + [KAl]Si_2O_6 = [CaAl]Si_2O_6 + [KMg]Si_2O_6. \quad (2)$$

The experimental results show that both isomorphic schemes, $Na^{M2} \rightleftharpoons K^{M2}$ and $Mg^{M1}Ca^{M2} \rightleftharpoons Al^{M1}K^{M2}$, are realized in the ternary solution *Di–Jd–KJd*. A combination of reactions (1) and (2) gives the hypothetical internal exchange equilibrium that is responsible for the influence of the jadeite end-member on $KAlSi_2O_6$ solubility in clinopyroxene, where Al and Mg occupy the M1 site:

$$[NaAl]Si_2O_6 + [KMg]Si_2O_6 = [KAl]Si_2O_6 + [NaMg]Si_2O_6. \quad (3)$$

The positive correlation between K and Mg in the M1 site and the negative correlation between K and Al in the same site (Figs. 4b, 4c) suggest a displacement of equilibrium (3) to the left ($\Delta G_{(3)} > 0$). Such a behavior is a direct consequence of the effect of acid–base interaction of components in solid solutions (Aranovich, 1991). In other words, according to schematic reaction (3), short-range order with Na–Al and K–Mg combinations is preferential in the clinopyroxene structure. However, the K–Mg combination is not charge-balanced and, therefore, unstable. An increase in K content in high-Na omphacite leads to accumulation of such unbalanced combinations. Thus, high potassium concentrations cannot be characteristic of jadeite-rich clinopyroxenes. In jadeite-poor clinopyroxenes, the displacement of internal exchange reaction (2) to the left is favorable for the formation of the $KAlSi_2O_6$ end-member in clinopyroxene and promotes a rapid increase in *KJd* solubility (Fig. 3a).

The change in the character of isomorphic substitutions that was observed in synthetic *KCpx* with varying jadeite content occurs also in natural clinopyroxenes. *KCpx* with the predominant $Mg^{M1}Ca^{M2} \rightleftharpoons Al^{M1}K^{M2}$ substitution was found as inclusions in garnet from the garnet–clinopyroxene rocks of the Kokchetav ultrahigh pressure complex, northern Kazakhstan (Sobolev and Shatsky, 1990; Perchuk *et al.*, 1996). These clinopyroxenes are characterized by very low Na_2O concentrations (below 0.5 wt %) and contain up to 1.5 wt % K_2O. The compositions of *KCpx* from these rocks vary in accordance with the isomorphic scheme $Mg^{M1}Ca^{M2} \rightleftharpoons Al^{M1}K^{M2}$, i.e., they show a positive correlation between K and Al and a negative correlation between K and Ca (Perchuk *et al.*, 1995, 1996). In contrast, most eclogitic *KCpx* from kimberlites and lamproites have very high Na_2O concentrations (up to 10 wt %), and their isomorphism is mainly of the $Na^{M2} \rightleftharpoons K^{M2}$ type. This feature of *KCpx* from kimberlites and lamproites is illustrated by Fig. 4a with data points of *KCpx* inclusions in diamonds from the Mir kimberlite pipe (Sobolev *et al.*, 1983), kimberlite pipes from Venezuela (Sobolev *et al.*, 1998), and the Argyle lamproite pipe (Jaques *et al.*, 1989). The compositional fields of these clinopyroxenes extend along the isobars.

The nonlinear increase of K content in clinopyroxenes with increasing pressure is also explained by a regular decrease in the volume of the M2 site (e.g., Levien and Prewitt, 1981), on the one hand, and decrease in the ionic radius of potassium (Montford and Swanson, 1965), on the other hand. It is possible that the above effect of the significant influence of pressure on potassium solubility in *KCpx* at 6–7 GPa is explained by the fact that the volume of the M2 polyhedron approaches that of the K ion in this pressure interval. This should enhance potassium incorporation into the omphacite structure. However, additional experimental and special X-ray studies are necessary to prove this effect.

Comparison of the Data Obtained with Independent Experimental Evidence on KCpx Synthesis

Our data for the dependence of potassium jadeite ($KAlSi_2O_6$) solubility in omphacite and jadeite on composition and pressure are in good agreement with some other experimental results on the synthesis of *KCpx* in various systems. This agreement was discussed above for the experimental data by Harlow (1997) for the 10 GPa isobar (Fig. 4b). Figure 4b shows *KCpx* analy-

ses synthesized in armalcolite–phlogopite lamproite melts at pressures of 5 and 6 GPa (Edgar and Vukadinovic, 1993) and sanidine–phlogopite lamproite at pressures of 5 and 7 GPa (Mitchell, 1995). These points are in good agreement with the isobars constructed on the base of our data.

However, not all experiments agree with the isobars in Fig. 4b. For example, data points for *KCpx* synthesized in the $Di_{50}Jd_{50}$ + *Kfs* system at 10 GPa (Harlow, 1999) are situated significantly lower than the corresponding isobar. The maximum K-jadeite content in clinopyroxene at given *P–T* conditions was probably not reached in this experiment. This suggestion is supported by the compositions of *KCpx* synthesized at 9.5 and 11 GPa, which plot near the 10 GPa isobar. Nevertheless, despite the difference in K and Na concentrations, the pyroxenes of the $Di_{50}Jd_{50}$ + *Kfs* system also show the limiting influence of jadeite end-member on the solubility of *KJd* in omphacite. Another example of a discrepancy between experimental data and the isobars in Fig. 4b is provided by clinopyroxenes synthesized in the melt of potassic basalt at pressures of 6–11 GPa (Tsuruta and Takahashi, 1998). These pyroxenes in equilibrium with the melt contain less than 0.01 f.u. of K and up to 0.4 f.u. of Na per 6 oxygen atoms. The reason for such inconsistency is low K_2O content in the coexisting melts (below 2.5 wt %), which prevents high potassium concentration in clinopyroxene.

The examples considered show that isobars in Fig. 4b are valid only for the conditions of clinopyroxene saturation with the potassium jadeite constituent. Under given *P–T* parameters, these conditions correspond to high bulk K_2O concentration.

Relations of Clinopyroxene and Aluminosilicate Melt

The major characteristics of melts coexisting with potassium-bearing omphacites in the system $CaMgSi_2O_6$–$NaAlSi_2O_6$–$KAlSi_2O_6$ are high contents of SiO_2, K_2O, and Al_2O_3 (Table 2). The compositions of these melts are comparable with those equilibrated with *KCpx* in the systems $Di_{50}Jd_{50}$–*Kfs* and *Di–Kfs–Ab* (Harlow, 1999). Noteworthy are very low Na_2O content and values of $K_p(Na_2O) \gg 1$, especially at 7 GPa (Table 2). The K_2O contents of the aluminosilicate melts coexisting with jadeite-poor and jadeite-rich *KCpx* are similar within the whole pressure range. The $K_p(K_2O) \ll 1$ values are much less than one and increase with increasing pressure. Thus, at constant *P* and *T*, omphacite crystallization from a melt enriched in both K_2O and Na_2O results in a significant displacement of the exchange equilibrium

$$NaAlSi_2O_6(L) + [KAl]Si_2O_6(KCpx) = KAlSi_2O_6(L) + [NaAl]Si_2O_6(KCpx) \quad (4)$$

to the right, i.e. to the formation of Na-rich clinopyroxene and K-rich melt.

The ability of sodic clinopyroxenes to limit the solubility of $KAlSi_2O_6$ at high pressures even at relatively low Na concentrations suggests that potassium-bearing omphacites could be formed from alkali-rich, mostly potassium-rich, melts. This case is illustrated by potassium-enriched (K_2O from 0.5 to 1.3 wt %) omphacite inclusions (Na_2O is up to 8 wt %) in diamonds from the Argyle lamproite pipe (Fig. 4a). Unfortunately, we have no information about melt inclusions in diamonds from these lamproites. However, the K_2O content of *KCpx* unambiguously reflects their precipitation from a potassium-rich melt. The compositional field of these clinopyroxenes is extended along the isobars. This suggests that the K_2O variations are related to the limiting influence of the jadeite component in omphacite rather than to pressure variations. According to Fig. 4a, pressure changed within the range 6–6.5 GPa.

Inclusions of aluminosilicate melts are rare in diamonds from kimberlites. Inclusions of potassic (up to 15 wt % K_2O) aluminosilicate melts with high Al_2O_3 and SiO_2 contents are known in diamonds from kimberlites (*e.g.*, Prinz *et al.*, 1975). Similar melt inclusions (up to 13–16 wt % K_2O) are associated with Na-rich omphacites (up to 6.5 wt % Na_2O) and garnet in diamonds from the Mir kimberlite pipe (Novgorodov *et al.*, 1990). Similar compositions of coexisting phases were produced in our experiments (Table 2). This allows their comparison. Figure 4a shows that the compositions of clinopyroxene inclusions correspond to the 5–6 GPa isobars. The presence of potassium feldspar among the phases of inclusions (Urakawa *et al.*, 1994) provides evidence for their equilibrium at a pressure below 6.5 GPa.

Inclusions of potassium-bearing omphacites in diamonds were described in association with inclusions of carbonate and brine fluids containing 25–35 wt % K_2O (*e.g.*, Izraeli *et al.*, 2001). The Na_2O content of these fluids is below 5 wt %. Unfortunately, there are no experimental data on potassium and sodium partitioning between clinopyroxene and brine at high pressure. However, the coexistence of jadeite-rich omphacite with ultrapotassic carbonate melt is in agreement with the results of experiments in clinopyroxene–carbonate melt systems (Harlow, 1997). In turn, these experiments provide additional constraints to the isobars shown in Figs. 3a, 4a, and 4b on the basis of our experiments in the aluminosilicate system. Thus, the isobars shown in Figs. 3a, 4a, and 4b can be applied to estimate the relative depth of crystallization of natural potassium-bearing omphacites from mantle aluminosilicate and carbonate–silicate melts enriched in K and Na.

CONCLUSIONS

Experiments in the system $CaMgSi_2O_6$–$NaAlSi_2O_6$–$KAlSi_2O_6$ in the pressure range 5–7 GPa and their comparison with results of previous experiments showed that the jadeite component limits the ability of deep-seated clinopyroxene to accommodate

potassium even in equilibrium with ultrapotassic melts. Neglecting this factor may result in a fallacious conclusion on the polybaric (multifacies) crystallization of clinopyroxenes with different potassium concentrations.

ACKNOWLEDGMENTS

The review and suggestions by A.V. Girnis (Institute of Geology of Ore Deposits, Petrography, Mineralogy, and Geochemistry, Russian Academy of Sciences) improved the manuscript. The authors are very grateful to L.P. Red'kina (Institute of Experimental Mineralogy, Russian Academy of Sciences) for the preparation of starting compounds, analysts E.V. Guseva and N.N. Korotaeva (Laboratory of electron microscopy and microprobe analysis of the Department of Petrology, Moscow State University), and D.A. Varlamov (Institute of Experimental Mineralogy, Russian Academy of Sciences) for help with microprobe analysis. This study was financially supported by the Russian Foundation for Basic Research, project nos. 01–05–64775, 03–05–06289 (to O.G. Safonov), 02–05–64684 (to Yu.A. Litvin), and 02–05–64025 (to L.L. Perchuk); the Program for Support of Young Scientists of the Russian Academy of Sciences; the Science Support Foundation (young scientist program); and the Europea Academia Foundation.

REFERENCES

1. L. Ya. Aranovich, *Mineral Equilibria in Multicomponent Solid Solutions* (Nauka, Moscow, 1991) [in Russian].
2. F. C. Bishop, J. V. Smith, and J. B. Dawson, Lithos, **11**, 155 (1978).
3. G. D. Bromiley and H. Keppler, EMPG-IX J. Conf. Abstracts **7** (1), 19 (2002).
4. L. T. Chudinovskikh, V. A. Zharikov, R. A. Ishbulatov, and Yu.A. Matveev, Dokl. Ross. Akad. Nauk **380**, 1 (2001) [Dokl. Earth Sci. **381**, 956 (2001)].
5. A. D. Edgar and R. H. Mitchell, J. Petrol. **38**, 457 (1997).
6. A. D. Edgar and D. Vukadinovic, Geochim. Cosmochim. Acta, **57**, 5063 (1993).
7. T. Gasparik, Contrib. Mineral. Petrol. **89**, 346 (1985).
8. M. R. Ghorbani and E. A. K. Middlemost, Am. Mineral. **85**, 1349 (2000).
9. D. L. Hamilton and C. M. B. Henderson, Mineral. Mag. **36**, 832 (1968).
10. G. E. Harlow, in *Proc. 7th Int. Kimberlite Conf., Cape Town, 1999*, Vol. 1, pp. 321–331.
11. G. E. Harlow, Am. Mineral. **82**, 259 (1997).
12. E. S. Israeli, J. W. Harris, and O. Navon, Earth Planet. Sci. Lett. **5807**, 1 (2001).
13. A. L. Jaques, A. E. Hall, J.D. Sheraton, *et al.*, in *Kimberlites and Related Rocks* (Geol. Soc. Austral. Spec. Publ., 1989), Vol. 14, pp. 966–989.
14. A. L. Jaques, H. St. C. O'Neill, C. B. Smith, *et al.*, Contrib. Mineral. Petrol. **104**, 255 (1990).
15. I. Kushiro, Carnegie Institution Year Book 64 (1965), pp. 112–117.
16. L. Levien and C. T. Prewitt, Am. Mineral. **66**, 315 (1981).
17. Yu. A. Litvin, *Physicochemical Studies on the Melting of the Earth's Deep-Seated Material* (Nauka, Moscow, 1991) [in Russian].
18. I. D. McGregor and J. L. Carter, Phys. Earth Planet. Inter. **3**, 391 (1970).
19. R. H. Mitchell, J. Petrol. **36**, 1455 (1995).
20. C. E. Montford and C. A. Swanson, Phys. Chem. Solids **26**, 291 (1965).
21. J. D. Moore and J. J. Gurney, Nature (London) **318**, 582 (1985).
22. P. G. Novgorodov, G. P. Bulanova, L. A. Pavlova, *et al.*, Dokl. Akad. Nauk SSSR **310** (2), 439 (1990).
23. L. L. Perchuk, O. G. Safonov, V. O. Yapaskurt, and J. M. Barton, Lithos **60** (3–4), 89 (2002).
24. L. L. Perchuk, N. V. Sobolev, V. O. Yapaskurt, and V. S. Shatskiĭ, Dokl. Ross. Akad. Nauk **348**, 790 (1996) [Dokl. Earth Sci. **349**, 737 (1996)].
25. L. L. Perchuk, V. O. Yapaskurt, and A. Okai, Petrologiya **3** (3), 267 (1995).
26. M. Prinz, D. V. Manson, P. F. Hlava, and K. Keil, Phys. Chem. Earth **9**, 797 (1975).
27. A. M. Reid, R. W. Brown, J. B. Dawson, *et al.*, Contrib. Mineral. Petrol. **58**, 203 (1976).
28. R. S. Ricard, J. W. Harris, J. J. Gurney, and P. Cardoso, in *Kimberlites and Related Rocks: Their Mantle/Crust Setting, Diamonds, and Diamond Exploration*, Ed. by J. Ross *et al.* (Blackwell Sci. Publ. Carlton, Victoria, Geol. Soc. Austral. Spec. Publ.) **2** (14), 1054 (1989).
29. O. G. Safonov, Yu. A. Matveev, Yu. A. Litvin, and L. L. Perchuk, Petrologiya **10**, 587 (2002) [Petrology **10**, 519 (2002)].
30. D. J. Schulze, J. V. Valley, and M. J. Spicuzza, Lithos **54**, 23 (2000).
31. H. Skogby, D. R. Bell, and G. R. Rossman, Am. Mineral. **75**, 764 (1990).
32. J. R. Smyth and C. J. Hatton, Earth Planet. Sci. Lett. **34**, 284 (1977).
33. J. R. Smyth, D. R. Bell, and G. R. Rossman, Nature (London) **351**, 732 (1991).
34. N. V. Sobolev and V. S. Shatsky, Nature (London) **343**, 742 (1990).
35. N. V. Sobolev, E. S. Efimova, and L. V. Usova, in *Mantle Xenoliths and the Problem of Ultramafic Magmas* (Nauka, Novosibirsk, 1983), pp. 4–16 [in Russian].
36. N. V. Sobolev, E. S. Yefimova, D. M. Channer de R., *et al.*, Geology **26** (11), 971 (1998).
37. T. Stachel, G. P. Brey, and J. W. Harris, Contrib. Mineral. Petrol. **140**, 1 (2000).
38. L. A. Taylor, G. A. Snyder, G. Crozaz, *et al.*, Earth Planet. Sci. Lett. **142**, 535 (1996).
39. K. Tsuruta and E. Takahashi, Phys. Earth Planet. Inter. **107**, 119 (1998).
40. S. Urakawa, T. Kondo, N. Igawa, *et al.*, Phys. Chem. Mineral. **21**, 387 (1994).
41. B. J. Wood, T. J. B. Holland, R. C. Newton, and O. J. Kleppa, Geochim. Cosmochim. Acta **44**, 1363 (1980).